J E M T
Journal of Earth and Marine Technology
homepage URL: ejurnal.itats.ac.id/jemt

# Seismic Vulnerability Evaluation in Western Bandar Lampung's Quarter Formation using the ERT Technique

Rustadi *[1], I Gede Boy Darmawan[2], Rudi Zefrianto Sinambela [3]
[1,2,3] Department of Geophysic Engineering, Universitas Lampung, Indonesia
*e-mail: rustadi.1972@eng.unila.ac.id

**Article info**
Received:
May 25, 2023
Revised:
Oct 7, 2023
Accepted:
Oct 8, 2023
Published:
Oct 14, 2023

**Keywords:**
ERT, Seismic hazard, Bandar Lampung

**Abstract**
Western Bandar Lampung is rapidly evolving into a sought-after residential locale and a scenic mountainous tourist spot. Notably, this region sits atop multiple fault structures, signaling potential seismic threats. This study aims to gauge the susceptibility of superficial layers by analyzing the resistivity properties of the underlying rock. Using the ERT geoelectric method across three lines, following the Wenner-Schlumberger configuration, a length of 140 m was mapped with electrodes spaced at intervals of 5 m. The subsurface materials in the examined area displayed a resistivity range between 4 and 1050 Ohm m, characterized by a blend of weathered constituents and igneous lenses. The dominant presence of extensively weathered material, especially given its thickness, highlights possible seismic dangers, including amplification, liquefaction, and potential landslides. To mitigate the repercussions of seismic hazards stemming from these fault lines, there is an imperative need for stringent adherence to construction guidelines tailored for seismically active regions.

## 1. Introduction

The western region of Bandar Lampung City is intrinsically linked to the broader Sumatra regional fault system (as shown in Figure 1a). This connection is evidenced by the volcanic activities that have led to the formation of Mount Ratai and Mount Betung. Historically, this region has been riddled with various fault lines, evidenced by a series of earthquakes in 2006 (illustrated in Figure 1b). Over a span of four months, recurrent low-magnitude earthquakes (MW < 5) were observed. By January 2021, similar seismic activities resurfaced across several fault segments, especially in the western region of Mount Ratai Pesawaran, adjacent to Mount Betung [1].

The Sumatra Fault presents a latent threat. Historical records pinpoint it as a catalyst for major disasters in multiple segments. For instance, in 1993, an earthquake proximate to the Bandar Lampung area registered an alarming magnitude of MW = 6.8. Another seismic event in the same segment within the West Lampung District escalated to a magnitude of MW = 7.0 [3,4]. The ramifications were dire during the earthquake of February 15, 1994, leading to severe infrastructural damages in Liwa. Tragically, 196 lives were lost, with injuries afflicting nearly 2,000 individuals. The tremor's aftermath left 75,000 residents without homes, with its impact resonating as far as 40 km from the West Lampung Regency's heart.

Western Sumatra Island, with its dynamic tectonic processes averaging subduction speeds of 6-7 cm/year, remains susceptible to fault deformations within the megathrust zone, leading to shifts across the Sumatra Fault's various segments (refer to Figure 1a). It's noteworthy that several known (and potentially unknown) faults in the western part of Bandar Lampung were reactivated in both 2006 and 2021, releasing seismic energy. The inherent character of the soil layers, or the "site class", is a focal point for researchers, especially concerning the varying responses to earthquake-induced vibrations. As these tremors travel, their surface interactions can produce diverse vibrations, largely contingent upon the varying soil layer densities. It is these vibrations within the soil strata that predominantly precipitate structural damages and collapses. Further complicating this is the presence of shallow

groundwater, which can instigate liquefaction phenomena [6-7] and potential landslides on steeper terrains [8].

Given the region's composition predominantly of youthful volcanic materials, seismic events such as those in Cugenang, Lombok, and Palu offer empirical evidence. Specifically, materials yet to undergo compaction can significantly amplify the resulting damage [9]. This research leverages the Electrical Tomography Resistivity (ERT) methodology to probe the shallow soil layers' composition, particularly in residential zones nestled at the base of Mount Betung. Although ERT doesn't directly evaluate the site class, it is instrumental in detecting water presence [10], which can be a precursor to both liquefaction and avalanches.

## 2. Regional Geology Setting

The intricate geological tapestry of Bandar Lampung has evolved due to the sustained tectonic activities on Sumatra Island since the pre-Tertiary era. Prolonged subduction phenomena have fostered a multifaceted geological framework in the region. The rugged topography of the Mount Betung volcanic complex further underscores the magmatic upsurge that ensues from plate interactions. This trajectory of volcanism, or magmatic arc, intersects with meta-sedimentary rocks, which in specific regions, have been uplifted and now lie at relatively shallow depths. The emergence of volcanic belts in Bandar Lampung's western corridor can be attributed to multiple identified fault lines, as delineated in Figure 1.

Mount Betung, which took shape during the Pliocene-Quaternary period, has played a pivotal role in shaping the geological architecture of western Bandar Lampung. The predominant geological feature in this vicinity is the Young Volcano Formation (Qhv), characterized by a composition of andesite-basalt lava and pyroclastic residues. The region showcases quintessential extrusive and intrusive igneous formations, often accompanied by volcanic ash deposition — a hallmark of volcanic terrains [11]. Notably, the thickness of the volcanic ash deposit layer tends to exert a more profound influence on the area's vulnerability than the inherent composition of crystalline rocks. The water content, which permeates the porous strata formed from pyroclastic accumulations, can also modulate the layer's structural integrity. Furthermore, the region's pronounced topographical gradients compound the susceptibility of the volcanic ash stratum to slippage during seismic activities.

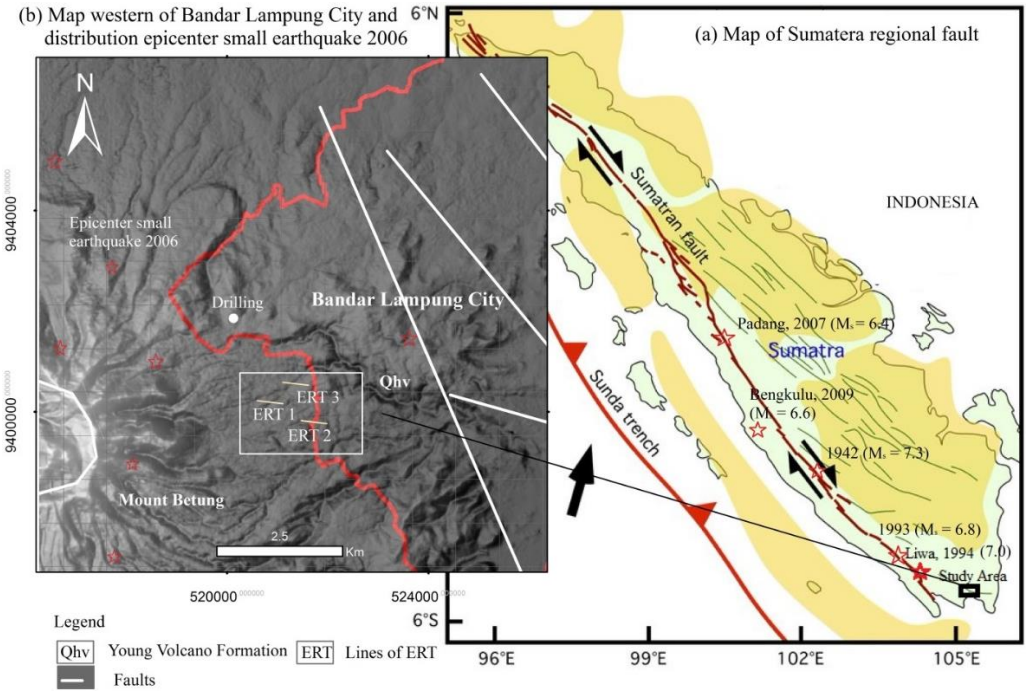


Figure 1. Geological map and the presence of structures in the eastern part of Bandar Lampung City. The red star represents the epicenter points of the 2006 earthquake. The red line in (b) is the regional boundary and the yellow line represents the ERT lines.

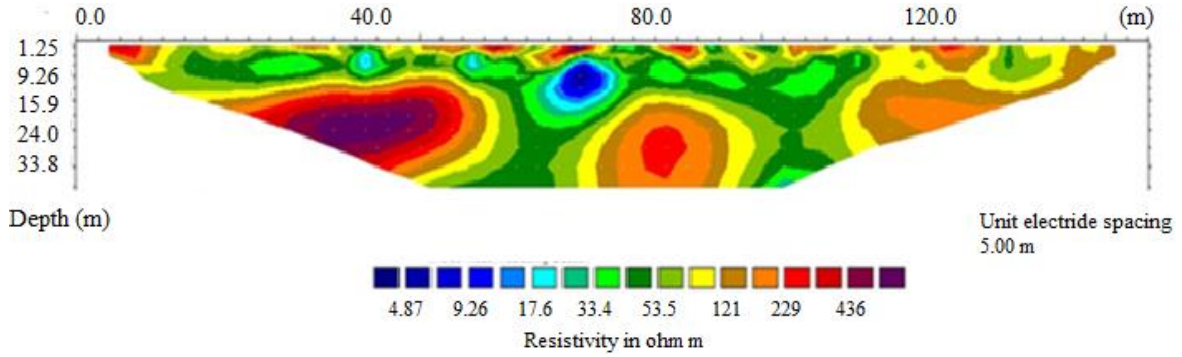


Figure 2. Subsurface resistivity image on ERT 1

## 3. Methodology

For effective mitigation, it's paramount to discern the load-bearing capacity of the near-surface soil or rock, especially within the depth range of 0–20 meters. The intrinsic properties of these soil or rock strata critically influence the structural resilience against seismic tremors. The structure's stability—ensuring it remains free from deformities like decomposition, liquefaction, or landslides—is contingent upon these layers functioning optimally as a foundational support. As visualized in Figure 1, three distinct ERT trajectories are employed to capture the soil's vulnerability. These measurements deploy the ARES instrumentation, utilizing the Wenner–Schlumberger configuration over a span of 140 m, maintaining an electrode spacing of 5 m.

The resistivity metric of the soil and rock directly correlates with their mineralogical composition and the fluid saturating the pore spaces. Notably, the extent of water infiltration within these spaces significantly impacts electrical conductivity. Varying fluid content, even within identical materials, can result in marked disparities in resistivity. Dry soil strata essentially function as resistive entities, showcasing resistivity values that considerably exceed those in water-saturated conditions. Drawing from laboratory analyses by Pandey, sand characterized by a uniform grain size and devoid of water demonstrates resistivity levels up to 500 Ohm m. However, this resistivity plunges with increasing moisture content, reaching a value of 60 Ohm m at 20% saturation [12-13].

Electrical resistivity tomography (ERT) is a hybrid technique, fusing the principles of traditional mapping and sounding methodologies [14-16]. Data points are laterally distributed via the strategic placement of both current and potential electrodes in a linear arrangement, with fixed intervals. These electrodes are then systematically realigned or shifted across the surface following a predetermined trajectory [17-18]. Sequential data sets for varying depths are sourced by adjusting the spacing between the electrodes. Each electrode positioning yields an apparent resistivity figure. The authentic resistivity value, however, is procured via model inversion, which offers a 2D cross-sectional representation of the subsurface, marked by material-specific resistivity metrics. Owing to its precision and versatility, the ERT approach finds extensive applications in delineating areas of intricate geological structures and evaluating soil vulnerability in geotechnical arenas [19–21].

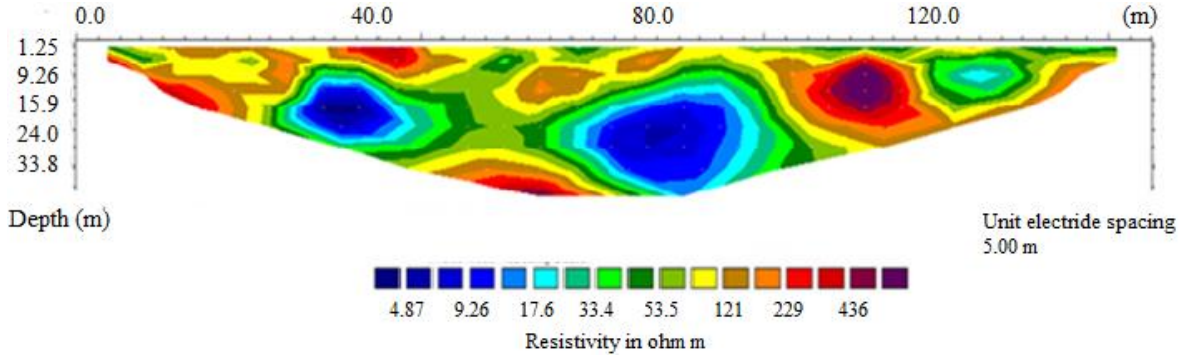


Figure 3. Subsurface resistivity image on ERT 2

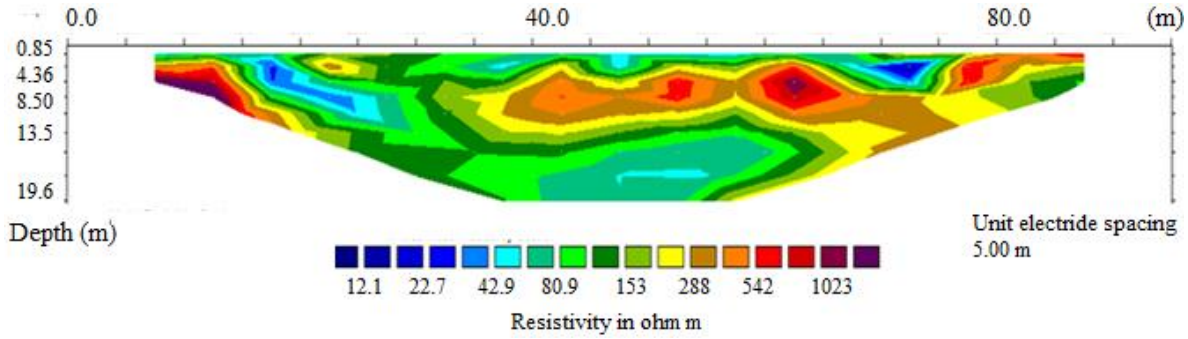

Figure 4. Subsurface resistivity image on ERT 3

## 4. Results and discussions

The subsurface configurations derived from the electrical resistivity tomography (ERT) within the volcanic path offer significant insights into the geological characteristics of the region, as detailed in Figures 2, 3, and 4. In the depths extending up to 33 m, ERT 1 and ERT 2 unveil a subsurface composition with resistivity values spanning from 4 - 440 Ohm m. ERT 3, which probes down to 19 m, indicates a broader spectrum of resistivity, ranging between 12 – 1050 Ohm m. This wide array of resistivity values is attributed to the volcanic environment dominated by a medley of igneous rock formations juxtaposed with the weathered remnants stemming from ancient pyroclastic events.

Conductive substrates with resistivity values below 60 Ohm m are presumably concoctions of water-saturated clay and interspersed sand lenses, acting as localized aquifers. It's interesting to note the behavior of dry clay which, once compacted, showcases resistivity values between 70 – 150 Ohm m. This is visually demarcated through a gradient transitioning from green to yellow. Materials with higher resistivity values, over 150 Ohm m, colored in shades of red, are likely representative of igneous rocks. These are solidified remnants of erstwhile lava flows, which cooled over time to yield extrusive rock forms. To further comprehend this geological tapestry, one can reference the drilling data showcased in Figure 1. Extracted from the northern measurement area, this drilling data portrays a layered journey through a slender pyroclastic sheet, a blend of clay and breccia, finally plunging into a dense core of andesite rock. It's fascinating how the sporadic distributions of breccia, indicative of shallow groundwater reservoirs, and the andesite pathways, are historical records. They whisper tales of the age-old volcanic activities of Mount Betung, recounting the sequence of formation of its extrusive and intrusive components.

Diving deeper into the profiles generated by the ERT scans, it becomes evident that the subsurface is a mosaic, a marriage between weathered artifacts and pockets of igneous rock intrusions. The inherent qualities of these materials determine their behavior during seismic activities. Igneous rocks, dense and sturdy, swiftly convey seismic tremors, acting as efficient conduits for these energy waves. Conversely, weathered sediments lag in this seismic transmission, their inherent loose structure making them susceptible to amplifying seismic vibrations, thus posing threats to human-made structures. This isn't the end of the challenges. The lurking presence of shallow groundwater can be a catalyst, potentially leading weathered fragments down the perilous path of liquefaction, especially in areas with pronounced inclines, potentially triggering landslides.

This region, with its unique geological narrative, naturally amplifies seismic waves, a behavior exacerbated by the vast expanses of weathered layers, some of which extend beyond 20 m in depth. The presence of aquifer lenses and pockets of shallow groundwater further intensifies the risks, especially in terms of liquefaction potential. Certain locales are characterized by formidable topographies, featuring steep inclines that exceed 40 degrees. Given these challenges, a robust mitigation strategy is paramount. Construction endeavors must align stringently with the building protocols designed for earthquake-prone regions, such as the rigorous Indonesian National Standards. Moreover, for sustainable habitation, it's imperative to identify and develop regions that offer stable terrains, thus circumventing the looming shadows of landslides and other geological threats.

## 5. Conclusion

The study area presents a diverse subsurface landscape with resistivity values ranging between 4 and 1050 Ohm m, intricately crafted by a blend of weathered materials and interspersed igneous rock formations. Predominantly characterized by extensive layers of weathered material, the region inherently possesses elevated risks associated with seismic activities, including amplification of seismic waves, potential liquefaction, and landslide hazards. To ensure the safety and resilience of infrastructures against these geological threats, it is imperative to adopt and rigorously enforce stringent building standards tailored for earthquake-prone regions. This not only necessitates a steadfast commitment but also a heightened community awareness to uphold these safety benchmarks.


## Acknowledgments

We wish to express our profound gratitude to the Department of Geophysical Engineering at Lampung University for their unwavering support and invaluable resources during the course of this research. We also recognize the contributions of the fieldwork team, whose dedication and hard work made the data collection seamless and efficient. The local community of Bandar Lampung deserves acknowledgment for their cooperation and assistance in facilitating our on-site studies. Lastly, we also deliver our acknowledgments to the JEMT reviewer who suggested us to improve our manuscript.


## References:


[1] I. Nurfitriana, A. Wibowo, and R. Rudianto, "Relokasi Gempa Bumi Swarm Di Pesawaran-Lampung, Januari 2021," *J. Geocelebes*, 2021, 91–101, 2021, doi: 10.20956/geocelebes.v5i1.13328.

[2] D. H. Natawidjaja, M. R. Daryono, G. Prasetya, Udrekh, P. L-F Liu, N. D. Hananto, W. Kongko, W. Triyoso, A. R. Puji, I. Meilano, E. Gunawan, P. Supendi, A. Pamumpuni, M. Irsyam, L. Faizal, S. Hidayati, B. Sapiie, M. A. and Kusuma, S. Tawil, "The 2018 Mw7.5 Palu 'supershear' earthquake ruptures geological fault's multisegment separated by large bends: Results from integrating field measurements, LiDAR, swath bathymetry and seismic-reflection data," *Geophys. J. Int*., 2021, 224,. 2,. 985–1002, doi: 10.1093/gji/ggaa498.

[3] Th. Duquesn, O. Bellier, M. Kasser,, M. Sebrier, Ch.Vigny, and I. Bahar, "Deformation related to the 1994 Liwa earthquake derived from geodetic measurements," *Geophysical Research Letters*, 1996, 23, 21, 3055-3058.

[4] C. Widiwijayanti, J. Devercheree, R. Louat , M. Sebriesr, H. Harjono, M. Diament, and D. Hidayat, "Aftershock sequence of the 1994, Mw 6.8, Liwa earthquake (Indonesia): Seismic rupture process in a volcanic arc," *Geophysical Research Letters*, 1996, 23, 21, 3051-3054.

[5] Syamsuddin, K. Sri Probopuspito, J. Sartohadi, W. Suryanto, and A. Moch Aryono, "Local Seismic Hazard Assessment of the Mataram City, Indonesia Based on Single Station Microtremor Measurement," *Int. Conf. Math. Sci. Educ*. 2014.

[6] R. Devi, R. G. Sastry, and N. K. Samadhiya, "Assessment of soil-liquefaction potential based on geoelectrical imaging: A case study," *Geophysics*, 2017, 82, 6, B231–B243, doi: 10.1190/GEO2017-0016.1.

[7] V. Lapenna and A. Perrone, "Time-Lapse Electrical Resistivity Tomography (TL-ERT) for Landslide Monitoring: Recent Advances and Future Directions," *Appl. Sci*., 2022, 12, 3, 2022, doi: 10.3390/app12031425.

[8] W. N. Tsai et al., "Electrical Resistivity Tomography (ERT) Monitoring for Landslides: Case Study in the Lantai Area, Yilan Taiping Mountain, Northeast Taiwan," *Front. Earth Sci*., 2021, 9, 1–17, doi: 10.3389/feart.2021.737271.

[9] T. R. Walter et al., "Soft volcanic sediments compound 2006 Java earthquake disaster," *Eos* (Washington. DC)., 2007, 88, 46, 486, doi: 10.1029/2007EO460002.

[10] I. Kongar, T. Rossetto, and S. Giovinazzi, "Evaluating simplified methods for liquefaction assessment for loss estimation," *Nat. Hazards Earth Syst. Sci*., 2017, 17, 5, 781–800, doi: 10.5194/nhess-17-781-2017.

[11] Rustadi, I. G. B. Darmawan, N. Haerudin, A. Setiawan, and Suharno, "Groundwater exploration using integrated geophysics method in hard rock terrains in Mount Betung Western Bandar Lampung, Indonesia," *J. Groundw. Sci. Eng*., 2022, 10, 1, 10–18, doi: 10.19637/j.cnki.2305-7068.2022.01.002.

[12] F. A. Kuranchie, S. K. Shukla, D. Habibi, X. Zhao, and M. Kazi, "Studies on electrical resistivity of Perth sand," *Int. J. Geotech. Eng.*, 2014, 8, 4, 449–457, doi: 10.1179/1939787913Y.0000000033.
[13] L. M. S. Pandey, S. K. Shukla, and D. Habibi, "Electrical resistivity of sandy soil," *Géotechnique Lett*., 2015, 5, 178–185, doi: 10.1680/jgele.15.00066.
[14] T. Dahlin and B. Zhou, "A numerical comparison of 2D resistivity imaging with 10 electrode arrays," *Geophys. Prospect*., 2004, 52, 5, 379–398, doi: 10.1111/j.1365-2478.2004.00423.x.
[15] T. Dahlin and B. Zhou, "Reply to Comment on: 'A numerical comparison of 2D resistivity imaging with 10 electrode arrays," *Geophys. Prospect*., 2005, 53, 6, 855–857, doi: 10.1111/j.1365-2478.2005.00509.x.
[16] T. Dahlin and B. Zhou, "Multiple-gradient array measurements for multichannel 2D resistivity imaging," *Near Surf. Geophys*., 2006, 4, 2, 113–123, doi: 10.3997/1873-0604.2005037.
[17] M. H. Loke and R. D. Barker, "Rapid least-squares inversion of apparent resistivity pseudosections by a quasi-Newton method," *Geophys. Prospect*., 1996, 44, 1, 131–152, 1996, doi: 10.1111/j.1365-2478.1996.tb00142.x.
[18] S. Idris, D. Darisma, A. H. Pramana, N. Aflah, M. Sayuti, and N. Novita, "Identification of the Aquifer Layer using the Geoelectric Method in Teupin Batee Village, Aceh Besar," *Bull. Comput. Sci. Electr. Eng*., 2022, 3, 1, 40–46.
[19] Y. Mertzanides, I. Tsakmakis, E. Kargiotis, and G. Sylaios, "Electrical resistivity tomography for spatiotemporal variations of soil moisture in a precision irrigation experiment," *Int. Agrophysics*, 2020, 34, 3, 309–319, doi: 10.31545/INTAGR/123943.
[20] M. Balasco, V. Lapenna, E. Rizzo, and L. Telesca, "Deep Electrical Resistivity Tomography for Geophysical Investigations: The State of the Art and Future Directions," *Geosci*., 2022, 12, 12, 1–19, doi: 10.3390/geosciences12120438.
[21] A. Aziz, R. Berndtsson, T. Attia, Y. Hamed, and T. Selim, "Noninvasive Monitoring of Subsurface Soil Conditions to Evaluate the Efficacy of Mole Drain in Heavy Clay Soils," *Water*, 2023, 15, 110, 1-16